Effect of formulation variables on the physical properties and stability of Dead Sea mud masks

SAWSAN SHAHIN, *SAJA HAMED,
and HATIM S. ALKHATIB, *Faculty of Pharmacy,
University of Jordan, Amman (S.S., H.S.A.), and Faculty of
Pharmaceutical Sciences, Hashemite University, Zarqa (S.H.), Jordan.*

Synopsis

The physical stability of Dead Sea mud mask formulations under different conditions and their rheological properties were evaluated as a function of the type and level of thickeners, level of the humectant, incorporation of ethanol, and mode of mud treatment. Formulations were evaluated in terms of visual appearance, pH, moisture content, spreadability, extrudability, separation, rate of drying at 32°C, and rheological properties. Prepared mud formulations and over-the-shelf products showed viscoplastic shear thinning behavior; satisfactory rheological behavior was observed with formulations containing a total concentration of thickeners less than 10% (w/w). Casson and Herschel–Bulkley models were found the most suitable to describe the rheological data of the prepared formulations. Thickener incorporation decreased phase separation and improved formulation stability. Bentonite incorporation in the mud prevented color changes during stability studies while glycerin improved spreadability. Addition of 5% (w/w) ethanol improved mud extrudability, slightly increased percent separation, accelerated drying at 32°C, and decreased viscosity and yield stress values. Different mud treatment techniques did not cause a clear behavioral change in the final mud preparation. $B_{10}G$ and K_5B_5G were labeled as "best formulas" based on having satisfactory physical and aesthetic criteria investigated in this study, while other formulations failed in one or more of the tests we have performed.

INTRODUCTION

The Dead Sea is the most concentrated hypersaline area in the world; it has an average salinity of 370 g salt per kilogram of water, compared with the ocean's average salinity of 35 g salt per kilogram of water (1). As the name indicates, this sea is devoid of life, except for salt-tolerant halophilic anaerobic bacteria (2).

Potassium chloride, magnesium chloride, calcium chloride, sodium chloride, and their corresponding bromides constitute the major salt components of the Dead Sea, comprising about 98% on a dry weight basis (3).

Address all correspondence to Saja Hamed at hamedsh@hu.edu.jo
*Current affiliation: Faculty of Pharmaceutical Sciences, Hashemite University, Zarqa, Jordan

Dead Sea mud is a suspension of very fine clay particles in water (4); it is the natural sediment of solid mineral clays with an interstitial solution of inorganic salts and sulfide compounds that arise from microbiological activity (5).

It is characterized by its blackish color and the distinct sulfur smell (1). In addition, at 25°C, it has a pH of 6.4–7.6, density of 1.6–1.8 g/l, water content of 30–40%, nonpathogenic microbial content of less than 100 CFU/g, and 86–98% of particles with size less than 5 mm (5).

The therapeutic effect of Dead Sea mud is related to its high mineral content and ability, due to its black color, to retain heat for many hours (3). In general, Dead Sea mud is used as packs for the treatment of rheumatic disorders such as myalgias, neuralgias, and osteoarthritis; masks to treat cutaneous skin disorders such as acne, dermatitis, psoriasis, xerosis, and eczema; and baths to treat lipodystrophy and cellulite (6,7).

In addition, Dead Sea mud and salts have been widely used in cosmetic and personal care products including lotions, masks, soaps, creams, and shampoos (1,3).

The formulation and processing of Dead Sea products is not a simple undertaking, and should be tackled using valid scientific and technical approaches. For example, the formulation of cosmetic emulsions containing Dead Sea salts is known to give rise to production and stability problems and development scientists must take into consideration the maximum salt level that can be incorporated into a formulation without affecting stability, consistency, and liquid phase separation while maintaining efficacy (8).

On surveying the commercially available Dead Sea mud mask products in the Jordanian market and interviewing technical and quality staff of Dead Sea products manufacturers, we have identified phase separation, stability issues as well as difficulty in processing, and filling as the major problems in this product category.

Rational use of formulation additives can improve the properties of mud formulations. These additives include thickeners that are expected to decrease phase separation of finished product, humectants that may be used to prevent dehydration, and ethanol that accelerates mud drying after application onto the skin.

This study was initiated to evaluate the effects of commonly used additives in Dead Sea mud formulations as well as mud treatment techniques on the physical properties, rheology, stability, and aesthetic acceptance of the finished mud products.

MATERIALS AND METHODS

MATERIALS

Dead Sea mud was provided by Numeira Mixed Salts & Mud Company Ltd. (Amman, Jordan), bentonite ($Al_2O_3.4SiO_2.H_2O$) was purchased from Vickers Laboratories Ltd. (West Yorkshire, England), kaolin ($Al_2H_4O_9Si_2$) was purchased from Merck (Darmstadt, Germany), Natrosol® 250 HHX (hydroxyethyl cellulose) was provided by Ashland Inc., (Wilmington, DE), and glycerin (99.5%) and ethanol pure (96%) were obtained from AZ-Chem (Selangor, Malaysia).

MUD PREPARATION

Effect of additives. Formulations were prepared using different concentration levels of thickeners [kaolin at 5%, 7.5%, 10%, 15% (w/w), bentonite at 2%, 5%, 7.5%, and 10% (w/w), and Natrosol® 250 HHX at 0.05% (w/w)] while glycerin was used as a humectant in some formulations at 10% (w/w) level.

Then, according to their aesthetics, ease of mixing and processing, and separation percentage, the most satisfactory formulas (shown in Table I) were chosen for further investigation.

Thickeners were incorporated into the mud by slow addition, as dry powder, over 15 min with continuous mixing using a planetary mixer (Home Electrics TC-800, China, 5.5 l capacity) at medium speed, then the whole preparation was left to mix for another 15 min to ensure homogeneity. When kaolin and bentonite were used in combination, kaolin was added first since it produced lower thickness than bentonite, and then bentonite was added.

Humectants were reported to prevent dehydration of the finished mud products on aging (9). Thus 10% glycerin was added to some of the studied Dead Sea mud mask formulations. Glycerin was incorporated by mixing with the mud for 5 min before the addition of the thickener as per the abovementioned procedure.

Ethanol was used at two concentration levels [(1% and 5% (w/w)] in selected formulations ($K_{15}G$, $B_{10}G$, K_5B_5G, K_5B_5, and $N_{0.05}G$). It was added as the final component to the mud mask mixture and mixed for an additional 5 min.

Five over-the-shelf Dead Sea mask products were selected to be studied parallel to our prepared formulations and were coded as RV, NC, BL, BS, and AQ. These samples were evaluated by the same procedures and at the same stability conditions as the prepared mud formulations.

The Dead Sea mud used in the above formulations was used as received without treatment except for the manual removal of stones (untreated mud).

Effect of mud treatment method. To investigate the effect of mud treatment method on the properties of Dead Sea mud formulations, the untreated mud was either dried in a tray

Table I
Compositions of the Selected Dead Sea Mud Mask Formulations Evaluated in the Stability Study

Formula code[a]	Composition percent (w/w)				
	Mud	Bentonite	Kaolin	Natrosol	Glycerin
$K_{15}G$	75	—	15	—	10
K_{10}	90	—	10	—	—
$B_{10}G$	80	10	—	—	10
K_5B_5G	80	5	5	—	10
$K_{7.5}B_{7.5}G$	75	7.5	7.5	—	10
K_5B_5	90	5	5	—	—
$N_{0.05}G$	89.95	—	—	0.05	10
$K_{10}B_2G$	78	2	10	—	10

[a]K = kaolin, B = bentonite, N = Natrosol® 250 HHX, G = glycerin. The subscript represents percent (w/w) level of the additive.

oven (Philip Harris Ltd, Shenstone, England) at 60°C for 72 h followed by milling and sieving through a 1-mm sieve to produce "dry powder" grade or by autoclaving the mud for 15 min at 121°C to produce "sterilized mud" grade.

Two formulas (K_{10} and K_5B_5G) were prepared using the treated mud (i.e., both dry powder and sterilized mud grades). These samples were evaluated by the same procedures and at the same stability conditions parallel to untreated mud formulations.

STABILITY STUDY

Formulations were stored in plastic jars under the following conditions and testing performed at the specified time points:

—Room temperature 25°C; analysis after the 14th and 28th days of storage.

—Elevated temperature 45°C; analysis after the 14th and 28th days of storage.

—Freeze–thaw cycling -20°C/24 h and room temperature/24 h; analysis after two temperature cycles.

The formulas were tested to provide a baseline value after 24 h of preparation to ensure complete hydration of the formulation. Samples stored at 45°C were left for 2 h at room temperature before testing and room temperature samples were considered as control samples.

Samples were evaluated visually, and tested for spreadability, extrudability, percent moisture content (w/w), rate of drying [percent (w/w)] at 32°C, pH, separation percent (w/w), and rheological properties.

Visual assessment. The visual appearance of all formulations evaluated during the study period included color, phase separation behavior, and any other distinct behavior.

Spreadability. The parallel plate method (10) was used to evaluate spreading behavior using an in-house spreadability testing apparatus that consisted of two smooth wooden slides to hold the mud samples and a pan to hold a weight during measurement as illustrated in Figure 1.
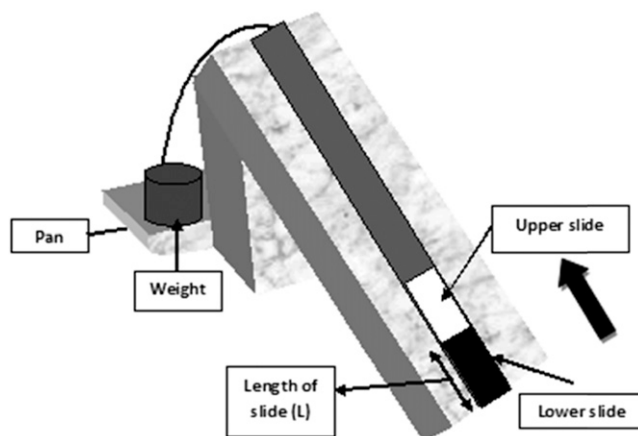

Figure 1. In-house spreadability testing apparatus used in the study.

Excess of the mud sample was spread on the surface of the lower slide, then the upper slide was used to cover the sample and a 100 g weight was used to compress the sample between the two slides for 2 min to obtain a layer of uniform thickness.

The time (in seconds) required for the upper slide to move away to the edge of the lower one when the 100 g weight is placed on the pan was recorded and spreadability was calculated using to the following equation

$$S = m \times \frac{l}{t} \qquad (1)$$

where S is the spreadability (kg cm·s^{-1}), m is the mass placed on the pan (0.1 kg), l is the length of the slide (cm), and t is the time (in seconds) required to move the upper slide (10). The test was performed in triplicates and data are presented as mean ± standard deviation (SD).

Extrudability. The extrudability was evaluated using the method described by Purushothamrao *et al.* (11) after modifications. The test was performed using a clean pouch (PET/PE, 500 g capacity) with a tip opening diameter of 1 cm. The pouch was half-filled with the mud formulation, then for each formulation the extrudability was evaluated in triplicate by measuring the weight of mud ejected from the pouch opening on pressing with fingers, while holding the pouch in hands. The test was performed in triplicates and data are presented as mean ± SD.

Percent moisture content (w/w). Duplicate measurements of percent moisture content (i.e., Loss on Drying percent; LOD%) were performed using a moisture analyzer (Adam AMB 310; Adam Equipment, Kingston, United Kingdom). The test was performed on 1–2 g samples at 60°C until a constant weight was achieved, and the percent moisture content was calculated as percent (w/w).

$$\% \text{ moisture content} = \frac{\text{initial weight} - \text{final weight}}{\text{initial weight}} \times 100 \qquad (2)$$

The test was performed in triplicates and data are presented as mean ± SD.

Drying rate at 32 °C. This test was performed to evaluate the drying behavior of different formulations under conditions mimicking the application of a mud mask onto human skin (12).

Accurately weighed samples of about 1 g were spread on square pieces of aluminum foil (5 × 5 cm) using a spatula to get a uniform layer. Samples were then placed in a laboratory incubator (IN-010; Gemmy Industrial Corporation, Taipei, Taiwan) maintained at 32° ± 1°C to simulate human skin temperature and monitored for 20 min, which is the application time suggested by manufacturers of facial mud masks.

Four samples were prepared from each tested formulation; one sample was withdrawn and weighed using an analytical balance (Shimadzu AY120 analytical balance; Nakagyo-ku, Kyoto, Japan) every 5 min up to 20 min. The drying percentage at each time point was calculated using the following equation

$$\% \text{ drying} = \frac{\text{original weight} - \text{weight after incubation}}{\text{original weight}} \times 100\% \qquad (3)$$

pH measurement. Mud dispersions [10% (w/w)] were prepared by adding deionized water to an accurately weighed amount of the tested formulation and leaving it to stir on a magnetic stirrer for 1 h (9). The pH of dispersions was measured using a microprocessor pH meter (Hanna pH 211; Woonsocket, RI).

Separation percent (w/w). The liquid phase separation percent for different formulations was evaluated using the method described by Zague *et al.* (9). The test was performed, in triplicates, by placing 15–20 g of the tested formulations in 15-ml centrifuge tubes that were centrifuged at 3500 rpm for 15 min (K2042; Centurion Scientific Ltd., Chichester, United Kingdom). The liquid supernatant was decanted and weighed. The separation percent (w/w) was calculated using the following equation

$$\text{Separation } \%\left(\text{w/w}\right) = \frac{\text{weight of separated liquid phase}}{\text{initial weight of sample}} \times 100 \qquad (4)$$

Rheological evaluation. The rheological properties of the mud formulations were studied using a Physica MCR 301 rheometer (Anton Paar, Austria) at 25°C using plate–plate system with a plate diameter of 25 mm and a gap of 1 mm. For each formulation, triplicate measurements of three different samples were performed for each of the rotational and oscillatory tests.

In the rotational tests, flow curves and viscosity curves were recorded in the shear rate range of 0–100·s^{-1}, then the obtained data were modeled using Casson and Herschel–Bulkley models shown in equations (5) and (6).

$$\text{Casson model: } \tau^{\frac{1}{2}} - \tau_c^{\frac{1}{2}} = \eta_c^{\frac{1}{2}} \times \dot{\gamma}^{\frac{1}{2}} \qquad (5)$$

where τ is the shear stress, τ_c is the Casson yield point, γ is the shear rate, and η_c is Casson infinite shear viscosity, which is the limiting value of viscosity at infinitely high shear rates (13).

$$\text{Herschel–Bulkley model: } \tau = \tau_{HB} + k \times \dot{\gamma}^n \qquad (6)$$

where τ is the shear stress, τ_{HB} is the Herschel–Bulkley yield point, k is the flow coefficient or consistency index, which serves as a viscosity index of the system, γ is the shear rate and the factor, n, is called the Herschel–Bulkley flow behavior index, which indicates the shear thinning tendency (14).

The following parameters derived from rotational testing were evaluated to compare the behavior of different formulations.

　　—Viscosity at different shear rate values (25/s and 75/s)

　　—Casson yield stress (Pa) and infinite shear rate viscosity (Pa·s) from the Casson model.

　　—Consistency index (Pa·s^n) and flow index (n) from the Herschel–Bulkley model.

Oscillatory test was performed at a constant angular frequency of 10·s^{-1} to obtain rheograms describing the linear viscoelastic range (LVE). The following parameters derived from oscillatory testing were used for evaluation and comparison purposes of the different formulations (15).

—Yield stress (Pa) at the limit of LVE

—Storage modulus (G′, Pa) at the limit of LVE

—Loss modulus (G″, Pa) at the limit of LVE

—Flow point (Pa): the stress value when (G′ = G″).

—Damping factor: the ratio of loss modulus to elastic modulus (G″/G′)

Data analysis. Data were summarized as mean ± SD; the mean value and SD values were calculated for a duplicate or triplicate measurements according to the methodology used.

Coefficient of determination (R^2) was used to evaluate the parameters (regression coefficients) calculated from both rheological models (Casson and Herschel–Bulkley models).

RESULTS AND DISCUSSION

PREPARATION OF DEAD SEA MUD MASK FORMULATIONS

Thickeners can change plasticity and alter the application characteristics of the finished product and are useful in stabilizing the dispersion of solids and preventing gradual phase separation, which is occasionally observed during the shelf life of clay masks (9).

Dead Sea mud mask formulations were prepared using three different thickeners (bentonite, kaolin, and Natrosol® 250 HHX), which were added to the mud in powdered form. This mode of addition was used as a way to disperse the thickener within the mud without having to increase its water content.

CHARACTERIZATION OF DEAD SEA MUD MASK FORMULATIONS

Visual assessment. Visual assessment results are described in Table II; samples varied in color from brown to dark gray and their consistency and thickness varied according to composition from easily extrudable formulations to thick formulations that were not easily extrudable.

Natrosol® 250 HHX produced samples with a gritty texture, which may be attributed to the incorporation technique used for slow addition and mixing of Natrosol® as dry powder to the mud, which may have been inadequate to cause efficient hydration and gelling of polymeric thickener.

Separation percent (w/w). Separation percent decreased for all prepared formulas as compared with the untreated mud except for $B_{10}G$ and $N_{0.05}G$, which showed separation values comparable to the untreated mud (Figure 2).

Separation percent for over-the-shelf formulations was generally higher than that of the in-house formulations. In comparison to the untreated mud, separation percent of over-the-shelf products was lower in the case of BL and RV only, while AQ, BS, and NC showed higher separation percent than the untreated mud.

Spreadability. Glycerin has been shown by our results (Figure 2) to be essential for formulation spreadability; formulations prepared without glycerin, K10, and K5B5 were not spreadable using the spreadability testing procedure used in this study (no movement using the 0.1 kg weight) as can be seen from the results in Figure 2.

Table II
Results of Visual Assessment, Spreadability, and Separation Tests for Formulations at Initial Time Point

Formula code[a]	Visual assessment	Spreadability (Kg cm·s^{-1})	Extrudability (g)	Separation percent (w/w)
Over-the-shelf samples				
RV	Faint brown color, thick texture, not easily extrudable	0.008 ± 0.001	4.10 ± 0.17	4.20 ± 0.35
BL	Dark gray and brown (nonhomogenous color), not easily extrudable	0.082 ± 0.011	3.45 ± 0.12	6.31 ± 0.29
NC	Dark gray color, easily extrudable	0.181 ± 0.006	6.02 ± 0.33	9.84 ± 0.45
BS	Faint brown color, easily extrudable	0.679 ± 0.186	4.75 ± 0.30	10.13 ± 0.11
AQ	Dark gray and brown (color variation), easily extrudable	0.963 ± 0.064	7.94 ± 0.54	13.57 ± 0.27
Stability samples				
Untreated mud	Gray-brown color, easily extrudable	0.053 ± 0.008	6.63 ± 0.12	8.85 ± 0.02
$K_{15}G$	Gray-brown color, thick, not easily extrudable	0.025 ± 0.003	5.40 ± 0.16	2.98 ± 0.41
K_{10}	Gray-brown color, very thick, not easily extrudable	No movement using the 100 g weight	6.61 ± 0.23	2.45 ± 0.49
$B_{10}G$	Dark gray color, easily extrudable	0.217 ± 0.043	9.17 ± 0.38	8.02 ± 0.52
K_5B_5G	Dark gray color, easily extrudable	0.099 ± 0.010	5.61 ± 0.27	4.99 ± 0.36
$K_{7.5}B_{7.5}G$	Dark gray color, easily extrudable	0.054 ± 0.007	14.25 ± 0.53	5.34 ± 0.47
K_5B_5	Gray-brown color, thick, and not easily extrudable	No movement using the 100 g weight	6.52 ± 0.21	4.26 ± 0.95
$N_{0.05}G$	Dark gray, gritty texture, acceptable extrudability	0.180 ± 0.022	7.66 ± 0.34	7.03 ± 0.88
$K_{10}B_2G$	Dark gray color, thick, and not easily extrudable	0.041 ± 0.004	5.63 ± 0.21	4.05 ± 0.45

Results represent mean ± SD (n = 3).
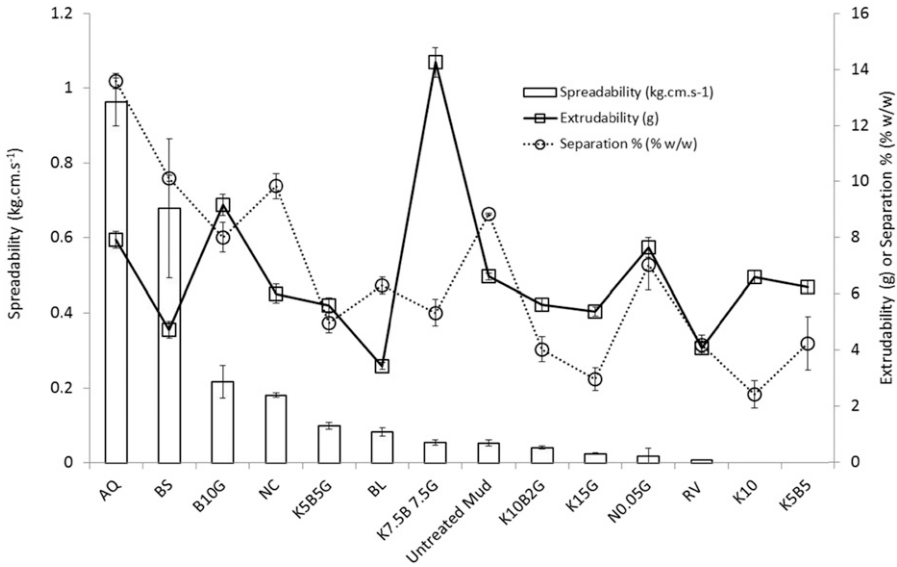[a]K = kaolin, B = bentonite, N = Natrosol® 250 HHX, G = glycerin, over-the-shelf brands = RV, NC, BL, BS, and AQ.

Figure 2. Separation percent, spreadability, and extrudability of tested samples at initial time point. Results represent mean ± SD (n = 3). K = kaolin, B = bentonite, N = Natrosol® 250 HHX, G = glycerin, over-the-shelf mud = RV, NC, BL, BS, and AQ.

Most formulations showed an improvement in their spreadability compared with untreated mud as shown in Figure 2. The best spreading behavior was for over-the-shelf products AQ, BS, and NC and the in-house $B_{10}G$, K_5B_5G, and $N_{0.05}G$. The spreadability ranking results were in agreement with subjective assessments.

Extrudability. Extrudability values are shown in Figure 2. The extrudability is an indicator of the amount of mud that the customer can eject from the pouch container. No correlation was found between ease of spreadability and the ejected amount; the samples that were thick and not spreadable resulted in extruded amounts comparable to those formulas that were easily spreadable.

Drying rate at 32 °C. The water loss of formulations at $32° ± 1°C$ was monitored over a period of 20 min after application onto an inert surface. The time was set based on usage instructions stated on the over-the-shelf mud products and the temperature was chosen to simulate that of the skin. The duration of the test was chosen based on the instructions for use in the label of the over-the-shelf products stating that the product is to be applied for 15–20 min on the skin before washing it.

Untreated mud showed a mass loss of 10% after 5 min and 20% after 10 min and did not dry further until the end of the test (20 min). Most formulations showed a drying percentage after 20 min comparable to that of the untreated mud. However, the rate of drying was slower, which could be attributed to the presence of the thickeners and the humectant.

Over-the-shelf products RV and BS showed the highest drying percentage after 20 min (28%), which could be explained by the fact that they were the only over-the-shelf products listing ethanol as a component.

Percent moisture content (w/w). It was noted that percent moisture content (w/w) was not affected by changing the formulation composition; the values were always comparable to that of the untreated mud.

Literature data state that the percent moisture content (w/w) (LOD%) of Dead Sea mud at 25°C ranges from 30% to 40% (5). The percent moisture content (w/w) of our preparations ranged from 32% to 37%, and the untreated mud had a value of 35%. On the other hand, over-the-shelf Dead Sea mud products had a percent moisture content (w/w) range of 34–41% and the highest values observed for RV and NC products.

pH. The pH value of the Dead Sea mud at 25°C was reported by Ma'or *et al.* as 6.4–7.6 (5). Our results show that the untreated mud had a pH of 8, whereas the pH of our formulations varied between 7.9 and 8.3. This slight difference in pH value could be attributed to the differences in the chemical composition of different mud samples collected from different sites.

Rheological evaluation. The flow curves were used to calculate the values of yield stress, viscosity, flow index, consistency index, flow point, storage modulus, and loss modulus of each tested formulation. The effect of additives on the different rheological parameters was investigated. Over-the-shelf brands were evaluated using the same methodology and characterized in terms of their rheological parameters. The rheological results are summarized in Table III.

Most samples showed a typical viscoplastic, shear thinning behavior. A typical behavior of formula $B_{10}G$ is shown in Figure 3.

Such a shear thinning or thixotropic behavior, in which the material will decrease in viscosity as the shear rate is increased or with progression of the shear time, decreases the load on machines during mixing and causes the material to flow easily during filling. In addition, thixotropic behavior will ensure efficient spreadability on skin and structural consistency regain after application (3), which contributes to the consumer aesthetic acceptance.

However, the rheological behavior of formulations $K_{15}G$, $K_{7.5}B_{7.5}G$, $K_{10}B_2G$, NC, and RV was different; they showed a shear thinning viscosity curve, while the flow curve behavior was not compatible with any of the known non-Newtonian material flow curves as depicted in Figure 4 showing the behavior of formulation $K_{7.5}B_{7.5}G$ as an example.

Flow curves were fitted to the Casson and Herschel–Bulkley models. These models are considered the most commonly used models for time-independent flow behaviors with yield stress (16).

It has been suggested that the rheological behavior of clay water suspensions is best described using Herschel–Bulkley model (17). The Herschel–Bulkley model has been used by Abu-Jdayil and Mohameed (3) to study the effect of temperature and time on the rheological properties of a Dead Sea mask formulation. This could be explained by considering the fact that the quality of the regression and fitting using Herschel–Bulkley model is expected to be better than that obtained using the Casson model due to the presence of larger number of regression parameters (three in the Herschel–Bulkley model compared to two in the Casson model) (14,16,18,19). In addition, the Casson model makes an assumption that the flow behavior index or exponent is a constant equal to "0.5."

Table III
Summary of Rheological Parameters for Formulations at Initial Time Point

Formula code	Casson yield stress (Pa)	Flow index	Consistency index (Pa·s^n)	Shear stress at the limit of LVE (Pa)	Storage modulus at the limit of LVE (Pa)	Loss modulus at the limit of LVE (Pa)	Damping factor	Flow point (PA)	Viscosity at different shear rate values (Pa·s)		
									$25 \cdot s^{-1}$	$75 \cdot s^{-1}$	Infinite shear viscosity
Over-the-shelf samples											
RV	–	–	–	77.10 ± 3.5	8.3E+04 ± 5.2E+04	2.6E+04 ± 1.4E+04	0.29 ± 0.03	186.5 ± 35.8	43.7 ± 2.9	8.14 ± 4.05	–
NC	391.1 (0.99)	–	–	10.74 ± 1.9	1.9E+04 ± 0.071E+04	5.3E+03 ± 0.078E+03	0.29 ± 0.01	45.3 ± 10.6	25.0 ± 5.3	9 ± 2.9	4.07 ± (0.99)
BS	332.1 (0.99)	0.32 (0.95)	103.3 (0.95)	29.25 ± 4.7	2.8E+04 ± 0.37E+04	5.9E+03 ± 0.26E+03	0.21 ± 0.02	69.4 ± 2.4	28.0 ± 12.4	11 ± 4.8	10.24 ± (0.99)
BL	434.4 (0.99)	0.37 (0.94)	143.2 (0.94)	46.90 ± 6.6	7.2E+04 ± 0.43E+04	1.8E+04 ± 0.11E+04	0.24 ± 0.00	142.5 ± 16.3	32.0 ± 3.7	10 ± 1.3	4.52 ± (0.99)
AQ	157.6 (0.99)	0.3 (0.96)	66.7 (0.96)	8.86 ± 3.2	8.2E+03 ± 1.5E+03	2.0E+03 ± 0.43E+03	0.25 ±0.01	30.95 ± 2.80	10.0 ± 2.9	4 ± 1.9	2.38 ± (0.99)
Stability samples											
Untreated mud	385.0 (0.99)	0.5 (0.97)	156.3 (0.97)	36.37 ± 5.5	4.4E+04 ± 1.3E+04	1.1E+04 ± 0.24E+04	0.26 ± 0.02	63.03 ± 0.70	38.0 ± 7.8	18 ± 5.3	13.26 ± (0.99)39
K$_{15}$G	–	–	–	88.5 ± 18.1	1.6E+05 ± 0.33E+05	4.3E+04 ± 0.85E+04	0.28 ± 0.00	171.3 ± 15.7	90.0 ± 5.6	17 ± 6.4	–
K$_{10}$	624.4 (0.99)	0.49 (0.99)	398.7 (0.99)	305.5 ± 6.4	6.0E+05 ± 0.26E+05	1.4E+05 ± 0.064E+05	0.24 ± 0.01	598.0 ± 70.7	52.0 ± 6.6	33 ± 6.3	23.7 ± (0.99)
B$_{10}$G	556.1 (0.99)	0.28 (0.98)	323.3 (0.98)	27.5 ± 10.1	3.6E+04 ± 1.4E+04	8.6E+03 ± 2.8E+03	0.25 ± 0.03	79.5 ± 17.5	36.0 ± 2.9	16 ± 1.4	8.95 ± (0.99)
K$_5$B$_5$G	239.6 (0.99)	0.33 (1.0)	391.6 (1.0)	42.20 ± 0.8	4.8E+04 ± 0.81E+04	1.3E+04 ± 0.23E+04	0.26 ±0.01	118.5 ± 9.2	47.0 ± 4.5	21 ± 1.3	20.11 ± (0.99)

Table III
Continued

Formula code	Casson yield stress (Pa)	Flow index	Consistency index (Pa·s^n)	Shear stress at the limit of LVE (Pa)	Storage modulus at the limit of LVE (Pa)	Loss modulus at the limit of LVE (Pa)	Damping factor	Flow point (PA)	Viscosity at different shear rate values (Pa·s)		
									25·s^{-1}	75·s^{-1}	Infinite shear viscosity
K$_{7.5}$B$_{7.5}$G	–	–	–	50.7 ± 17	8.3E+04 ± 1.6E+04	2.2E+04 ± 0.4E+04	0.26 ± 0.00	123.0 ± 14.0	56.0 ± 1.1	9. ± 1.4	–
K$_5$B$_5$	567.5 (0.99)	0.42 (0.95)	236.8 (0.95)	206.0 ± 72	3.1E+05 ± 0.62E+05	7.5E+04 ± 1.9E+04	0.24 ± 0.02	410.3 ± 60.1	43.0 ± 2.9	24 ± 8.2	13.5 ± (0.99)
N$_{0.05}$G	713.2 (0.98)	0.26 (0.98)	395.5 (0.98)	101.6 ± 41.7	1.1E+05 ± 0.58E+05	2.8E+04 ± 1.4E+04	0.27 ± 0.02	246.3 ± 58.8	44.0 ± 7.9	13 ± 0.25	6.16 ± (0.98)
K$_{10}$B$_2$G	–	0.07 (1.0)	604.8 (1.0)	93.9 ± 28.4	1.4E+05 ± 0.15E+05	3.3E+04 ± 0.14E+04	0.24 ± 0.04	153.0 ± 15.6	59.0 ± 0.9	11 ± 4.7	–

[a]K = kaolin, B = bentonite, N = Natrosol® 250 HHX, G = glycerin, over-the-shelf mud = RV, NC, BL, BS, and AQ. Results represent the mean ± SD or mean (R^2) for parameters calculated using Casson and Herschel–Bulkley models (n = 3). For samples RV, NC, K$_{15}$G, K$_{7.5}$B$_{7.5}$G, and K$_{10}$B$_2$G; the models are not applicable to data, results make no sense rheologically.
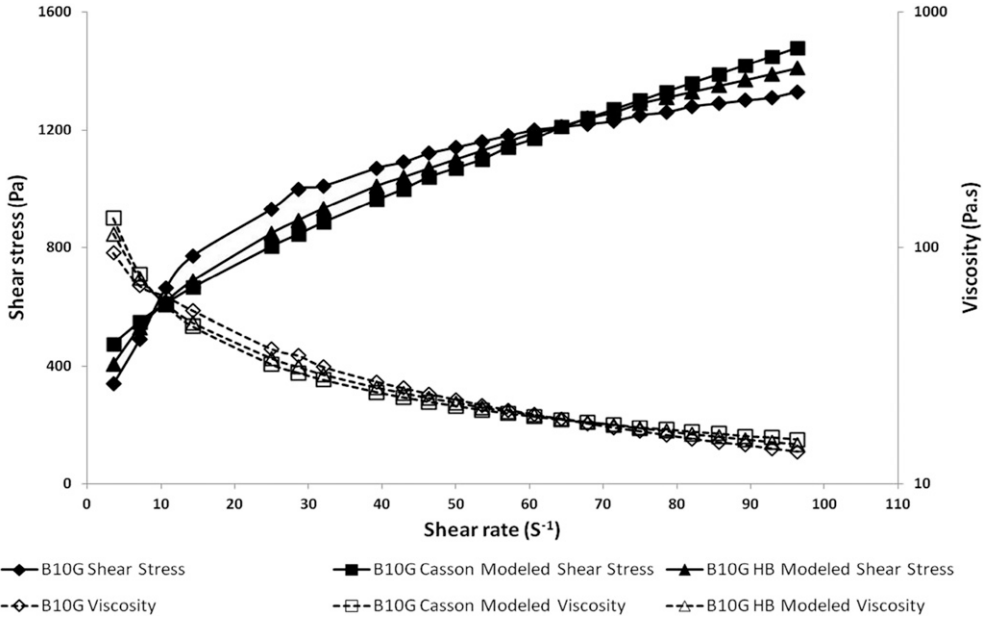
Figure 3. Typical shapes of Casson and Herschel–Bulkley (HB) modeled flow curves, data shown are for $B_{10}G$ at initial time (first day) point compared with unmodeled flow of the same formulation sample.

However, when our data were fitted to the Herschel–Bulkley model, we faced a problem of meaningless negative yield stress values for many of the samples, which include AQ, BL, BS, NC, $K_{15}G$, $K_{7.5}B_{7.5}G$, K_5B_5, $N_{0.05}G$, and $K_{10}B_2G$.
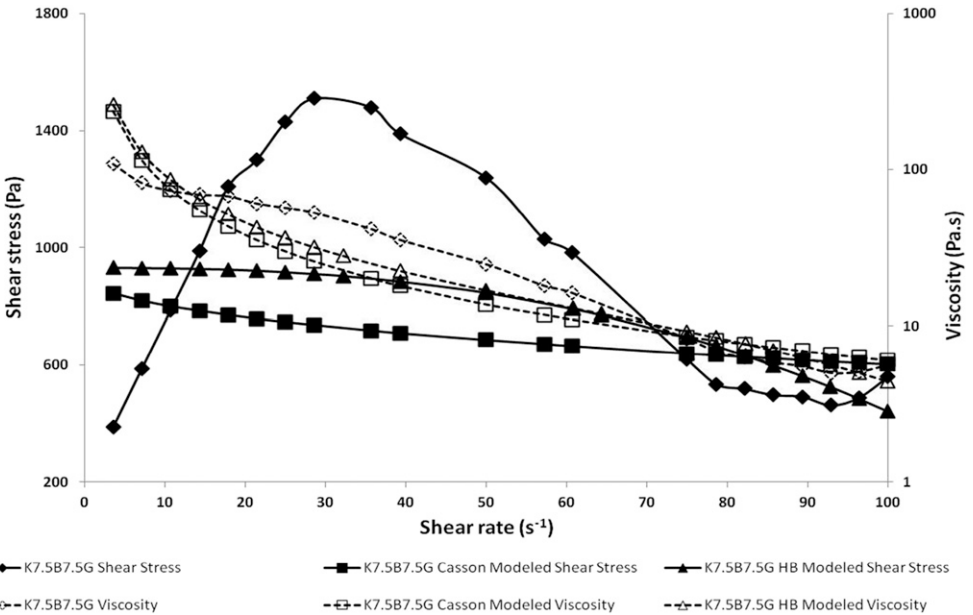

Figure 4. Casson and Herschel–Bulkley (HB) modeled flow curves for $K_{7.5}B_{7.5}G$ at initial time point compared with observed flow curves of the same formulation.

Several procedures can be followed to overcome the problem of negative meaningless yield stress values (18), the most applicable one for our samples involves using the Casson model to calculate yield stress for all samples and incorporated the calculated yield stress to the Herschel–Bulkley model and used it to fit the data to calculate both consistency and flow indices.

All formulations fitted to both models with high R^2 values except $K_{15}G, K_{7.5}B_{7.5}G$, $K_{10}B_2G$, RV, and NC, which had negative meaningless values for all or some of the parameters; yield stress value (either Casson, Herschel–Bulkley, or both), consistency index, flow index, and infinite shear viscosity. The behavior of $K_{15}G$, $K_{7.5}B_{7.5}G$, and RV did not fit either model, whereas that of NC fitted to Casson model only and $K_{10}B_2G$ fitted to Herschel–Bulkley model only as shown in Table III.

Correlating this deviated behavior with formulation composition revealed that the maximum level of thickener concentration that can be incorporated into a mud formulation without producing a deviation from the ideal shear thinning flow curves is 10% of either one thickener (kaolin and bentonite) or a combination of the two of them.

Casson yield stress values for our formulations were higher than that of the over-the-shelf samples; the highest was that of $N_{0.05}G$. All in-house prepared formulations mentioned in Table I had higher Casson yield stress compared with untreated mud, except K_5B_5G. While only BL from over-the-shelf products had higher value than the untreated mud.

Yield stress is the minimum shear stress required to initiate material flow. It is an important determinant of the product stability and the ease of product application by the end user (20).

Higher yield values ensure that the material will preserve its structure and consistency and maintain particles in the medium with minimal sedimentation (20). On the other hand, lower yield stress guarantees easier distribution of a semisolid on the skin and easier extrusion out of its tube (21).

An optimum yield stress value is required to balance between the ability to pump and fill the product and the stability during transfer and storage (3).

Consistency index values were comparable for most of our stability samples (300–400 Pa·s^n), the highest was that of $N_{0.05}G$ and K_{10} and the lowest was that of K_5B_5.

All in-house prepared formulations included in the stability study had higher values of consistency index compared with the untreated mud, except $K_{15}G$ and $K_{7.5}B_{7.5}G$ for which could not calculate the consistency index.

The consistency index is an indicator of structural strength and serves as an index of the viscosity of the system (14), and when the formulation consistency index is higher, the formulation viscosity, thickness, and yield stress are higher and the lower spreadability is lower.

The consistency index of the prepared in-house formulations was higher than that of the over-the-shelf products; the lowest value was for AQ brand.

Flow index values, an index of the shear thinning tendency of the samples (14), were less than one for all tested samples, which is an indicator of a shear thinning behavior (13).

Viscosity value differences were more obvious at lower shear rate (25 s^{-1}) than higher shear rate (75 s^{-1}). The highest viscosities were for $K_{15}G$, $K_{10}B_2G$, $K_{7.5}B_{7.5}G$, and K_{10}, while over-the-shelf products had the lower values.

Oscillatory test parameter values include yield stress at LVE limit, storage modulus, loss modulus, and flow point were generally higher for our in-house formulations than NC, BS, AQ, and BL of the over-the-shelf products, while RV had values comparable to in-house formulations. Highest values were for K_{10}, K_5B_5, and $N_{0.05}G$, while the lowest were for AQ and NC.

The storage modulus (G′) is the energy stored per unit volume, which is proportional to elastic component magnitude in the system contributed by cross-linking and/or aggregation, while the loss modulus (G″) is the energy dissipated per unit volume, which is proportional to the extent of the viscous component contributed by the liquid-like portions. The ratio of G″/G′ indicates the strength of interaction of the internal structure and it is called the damping factor (20).

The values of the storage modulus were higher than those of the loss modulus for all tested samples, which is a property of elastic systems. The ratio of loss modulus to storage modulus, expressed as the damping factor, was comparable for all samples (ranging from 0.21 to 0.29).

Higher formulation elasticity (higher storage modulus values) indicates a higher formulation thickness and yield stress and, consequently, a lower spreadability.

Shear stress and storage modulus values for in-house samples were all higher than the untreated mud, except for $B_{10}G$. On the other hand, over-the-shelf products had lower values than the untreated mud, except for RV and BL, which had higher values.

A flow point is the stress value when G′ = G″, which indicates the stress that will cause structural destruction of the material and consequent material flow (15). The higher the flow point, the higher stress required to cause material destruction, which could indicate higher product stability over its shelf life. On the other hand, it indicates higher yield stress values and lower spreadability.

Only NC and AQ had lower flow point values than untreated mud, the remaining over-the-shelf products and all of in-house formulations had higher values than untreated mud.

STABILITY OF DEAD SEA MUD MASK FORMULATIONS ON EXPOSURE TO STRESS CONDITIONS

The behavior of formulations listed in Table I and stored in plastic jars was investigated on exposure to elevated temperature of 45°C for a period of 4 weeks (accelerated stability study conditions) and freeze–thaw cycling. Samples stored at room temperature (25°C) were used as control samples.

Appearance. During stability studies, some formulations showed changes in its appearance at different storage conditions and different time points. Two samples from over-the-shelf products (AQ and BL) had color changes to rusty red after 2 weeks of storage at both room temperature and accelerated conditions, which increased more after 4 weeks at the same conditions.

On the other hand, only one formulation (K_{10}) showed color changes to brown and rusty red at room temperature conditions after 4 weeks, and a similar behavior was shown at accelerated conditions, but started after 2 weeks of storage, a rusty red color was observed.

Formulations $K_{15}G$, K_5B_5, $N_{0.05}G$, and $K_{10}B_2G$ showed no color changes at room temperature, while color changes appeared at accelerated conditions after 2 weeks of storage; slight brown color appeared that changed after 4 weeks at the same conditions into a rusty red color for formulations $K_{15}G$ and K_5B_5 and remained brown for the other two formulations. In addition, K_5B_5G started color changes to a very slightly brownish color after 4 weeks at only accelerated storage conditions.

Untreated mud showed a rusty red color after 4 weeks of storage at room temperature while the same changes started after 2 weeks of storage at accelerated conditions.

It was noticed that color changes occurred in formulations without hydrated aluminum silicate thickeners (kaolin and bentonite) and those containing kaolin as the sole thickener. The presence of bentonite alone or combined with kaolin at the same concentration level reduced the degree of color changes. This could be related to the high adsorption capacity of these materials that could bind whatever species responsible for color development, which may include iron compounds or carotenoids from *Dunaliella* (22).

Separation percent (w/w). The separation percent test that was used as a tool in formulation screening at the initial development stages (13) was also used to follow up changes throughout stability study. Significant changes in separation percent indicate early product failure on the shelf after marketing.

The most acceptable formulations at initial time point were NC, BS, BL, $B_{10}G$, K_5B_5G, $K_{7.5}B_{7.5}G$, and $N_{0.05}G$, which were characterized by moderate separation percent (5–10%).

AQ was the only one formulation that has extensive separation (>10%), whereas RV, $K_{15}G$, K_{10}, K_5B_5, and $K_{10}B_2G$ resulted in minimal separation percent; however, they were thick and not easily spreadable.

Separation percent was affected by storage at different conditions, the behavior of most samples was a decrease in separation percent during stability at both room temperature and accelerated conditions, but it was more notable at accelerated conditions; all samples showed a decrease in separation percent at accelerated conditions, which was also notable in visual assessment of samples as a change in product texture to a thicker one. The decrease in separation percent most probably attributed to the loss of water from the formulations during storage.

Separation behavior after freeze–thaw testing was not clear; some samples showed an increase in separation percent (RV, NC, BL, $K_{15}G$, K_{10}, K_5B_5G, and $K_{10}B_2G$), whereas the remaining formulations (BS, AQ, $B_{10}G$, $K_{7.5}B_{7.5}G$, K_5B_5, and $N_{0.05}G$) showed a decrease in separation after freeze–thaw cycles.

pH values ranged from 7.93 to 8.32 at initial time point and during stability study there was slight variation in pH values (maximum pH change was 0.3 units).

Rheological evaluation. Flow curves of $K_{15}G$, $K_{7.5}B_{7.5}G$, $K_{10}B_2G$, NC, and RV remained deviated from typical behavior at all the time points and different stability conditions, similar to their behavior at initial time point.

The main change in Casson yield stress values during stability was the notable increase at accelerated conditions, while only a slight change was noticed at room temperature storage. Some samples, BL and $N_{0.05}G$, showed a decrease in yield stress on storage under accelerated conditions. In addition, viscosity and oscillatory test parameter values increased during stability study at accelerated conditions.

A change in this rheological behavior during stability storage at different conditions constitute a direct indicative parameter of structure and consistency changes, and gives an early expectation of product instability over its shelf life (8). The increase in most rheological parameters at accelerated testing indicates the stability of these formulations and the minimal risk of product separation over its shelf life.

On the other hand, no changes were observed in flow index values during stability, which indicates that all formulations preserved their shear thinning behavior during stability testing, at all time points and under all storage conditions. Shear thinning is the target behavior for a semisolid mud preparation as discussed earlier.

The increase in most rheological parameter values and the decrease in separation percent could be attributed to the poor barrier efficiency of the package used, which could cause loss of water and volatile solvents during storage period and change product texture.

Freeze–thaw cycling. Freeze–thaw cycling did not produce clear correlations for all physical characterization tests. There was variation in separation and rheological values for different samples whereas pH and visual appearance remained the same.

EFFECT OF ETHANOL

The effect of ethanol addition was more obvious at the concentration level of 5%. Although it improved the extrudability and the aesthetic appearance of samples, it also decreased the yield stress and viscosity values as shown in Figure 5 for formulation K_5B_5, as an example. The flow index values of all samples were less than one, which indicates a shear thinning behavior.
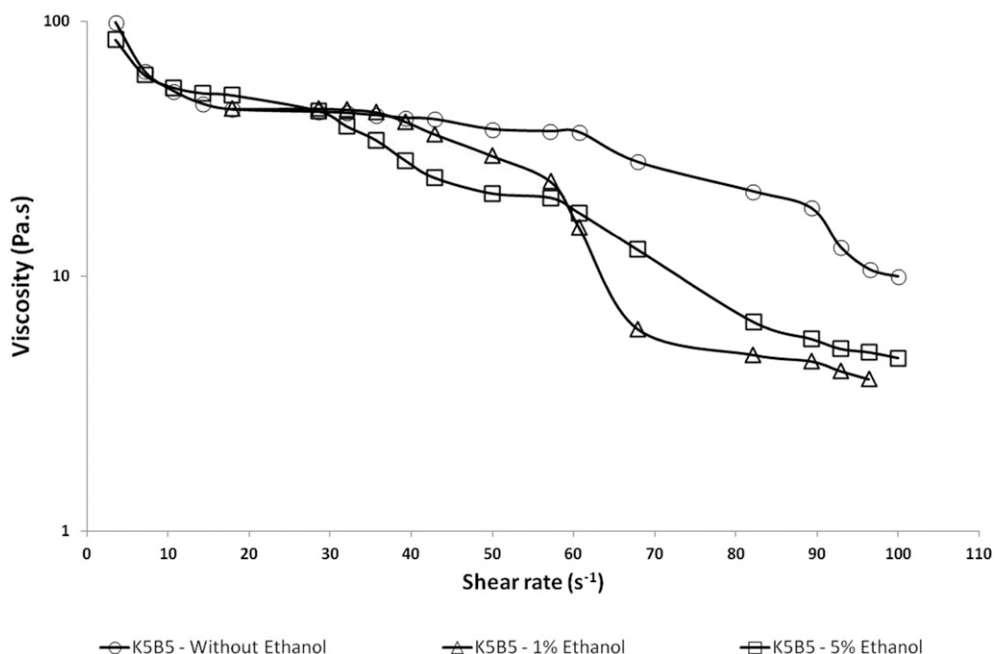

Figure 5. Effect of ethanol on the viscosity curves of K_5B_5 at initial time point.

In addition, ethanol incorporation improved drying percent of formulations slightly by 2–4%. For example, the drying percent for formulation $B_{10}G$ after 20 min was 16% (w/w). When ethanol 1% was added to the formulation, the drying percent after 20 min became 18% (w/w), while the addition of 5% ethanol resulted in 20% (w/w) drying percent after 20 min.

On the other hand, there was no clear correlation between ethanol addition and spreadability results. Extrudability values increased by 5–10% at initial time point when 5% (w/w) ethanol was added to the formulations, except formulation K_5B_5G, which did not show any change in extrudability values after ethanol incorporation into the formulation.

Separation percent increased by 2–4% and loss on drying percent values increased by 1–4% at initial time point when 5% (w/w) ethanol was added to the formulations, while pH changes were not significant. Table IV summarizes the effect of ethanol incorporation into in-house formulations on the results of separation, pH, spreadability, extrudability, and loss on drying tests.

Changes during stability study were similar to the changes happened for formulations without ethanol in their composition; values of oscillatory tests increased during stability at both room temperature and accelerated conditions. The apparent change in the results of yield stress and consistency index was an increase in their values at accelerated conditions.

In addition, the separation percent results changed on stability and the trend in most samples was a decrease in separation percent at different stability conditions, except K_5B_5G, which had an increase in separation during stability.

Changes in appearance at different storage conditions were similar to those noticed for samples without ethanol. $K_{15}G$, K_5B_5, and $N_{0.05}G$ had color changes even when ethanol was incorporated in the formulation composition, while $B_{10}G$ and K_5B_5G were stable.

EFFECT OF DIFFERENT MUD TREATMENT TECHNIQUES

Different mud treatment techniques did not cause a clear behavioral change neither at initial time point nor during stability testing, except for the fact that preparations made from the "dry powder" grade had a faint brown color rather than dark gray and higher pH values than those prepared from "untreated mud."

CORRELATION BETWEEN DIFFERENT PHYSICAL CHARACTERIZATION PARAMETERS

A linear correlation was observed between the storage modulus and yield stress values at the limit of LVE as shown in Figure 6.

Figure 7A and B show the correlation between spreadability and rheological parameters, and Figure 8A, B, and C show the correlation between separation percent and rheological parameters.

It is noticed from the figures that higher the formulation elasticity (higher storage modulus values), higher the formulation thickness and yield stress values, and, consequently, lower the spreadability and separation percent values.

Table IV
Summary of Separation, pH, Spreadability, Extrudability, and Loss on Drying Testing Results for the in-House Formulations Containing Ethanol at Different Concentration Levels, at Initial Time Point

Formula code[a]	Separation percent (w/w)	pH	Spreadability (kg·cm·s^{-1})	Extrudability (g)	LOD percent (w/w)
Mud without additives	8.85 ± 0.02	7.97 ± 0.02	0.053 ± 0.008	6.63 ± 0.12	35.25 ± 0.78
K$_{15}$G	2.98 ± 0.41	8.12 ± 0.03	0.025 ± 0.003	5.40 ± 0.16	33.00 ± 0.29
K$_{15}$G—containing 1% ethanol	4.64 ± 0.20	7.99 ± 0.01	0.059 ± 0.007	5.47 ± 0.28	32.44 ± 0.34
K$_{15}$G—containing 5% ethanol	6.80 ± 0.90	8.04 ± 0.03	0.029 ± 0.002	15.72 ± 0.40	36.72 ± 0.13
B$_{10}$G	8.02 ± 0.52	7.93 ± 0.03	0.217 ± 0.043	9.17 ± 0.38	35.75 ± 0.19
B$_{10}$G—containing 1% ethanol	7.37 ± 0.57	7.88 ± 0.02	0.107±0.009	9.17 ± 0.38	36.83 ± 0.57
B$_{10}$G—containing 5% ethanol	11.09 ± 0.07	8.01 ± 0.01	0.255 ± 0.054	14.63 ± 0.21	37.84 ± 0.03
K$_5$B$_5$G	4.99±0.36	8.24 ± 0.03	0.099 ± 0.010	5.61 ± 0.27	35.83 ± 0.39
K$_5$B$_5$G—containing 1% ethanol	5.46 ± 0.45	8.23 ± 0.08	0.277 ± 0.027	5.96 ± 0.23	37.01 ± 0.08
K$_5$B$_5$G—containing 5% ethanol	8.66 ± 0.25	8.20 ± 0.01	0.250 ± 0.035	6.30 ± 0.17	38.14 ± 0.81
K$_5$B$_5$	4.26 ± 0.95	8.02 ± 0.01	No movement	6.52 ± 0.21	32.45 ± 0.06
K$_5$B$_5$—containing 1% ethanol	4.46 ± 0.24	8.00 ± 0.01	No movement	6.01 ± 0.22	32.66 ± 0.45
K$_5$B$_5$—containing 5% ethanol	5.98 ± 0.36	7.97 ± 0.01	0.114 ± 0.016	11.10 ± 0.46	34.96 ± 0.35
N$_{0.05}$G	7.03 ± 0.88	8.32 ± 0.01	0.180 ± 0.022	7.66 ± 0.34	36.93 ± 0.67
N$_{0.05}$G—containing 1% ethanol	6.97 ± 0.78	8.28 ± 0.03	0.122 ± 0.011	13.70 ± 0.53	36.19 ± 0.69
N$_{0.05}$G—containing 5% ethanol	8.90 ± 0.30	8.15 ± 0.07	0.066 ± 0.003	15.40 ± 0.47	37.59 ± 0.36

Results represent mean ± SD (n = 3; for separation percent, spreadability and extrudability tests and n = 2; for LOD percent and pH tests).
[a]K = kaolin, B = bentonite, N = Natrosol 250 HHX, G = glycerin.
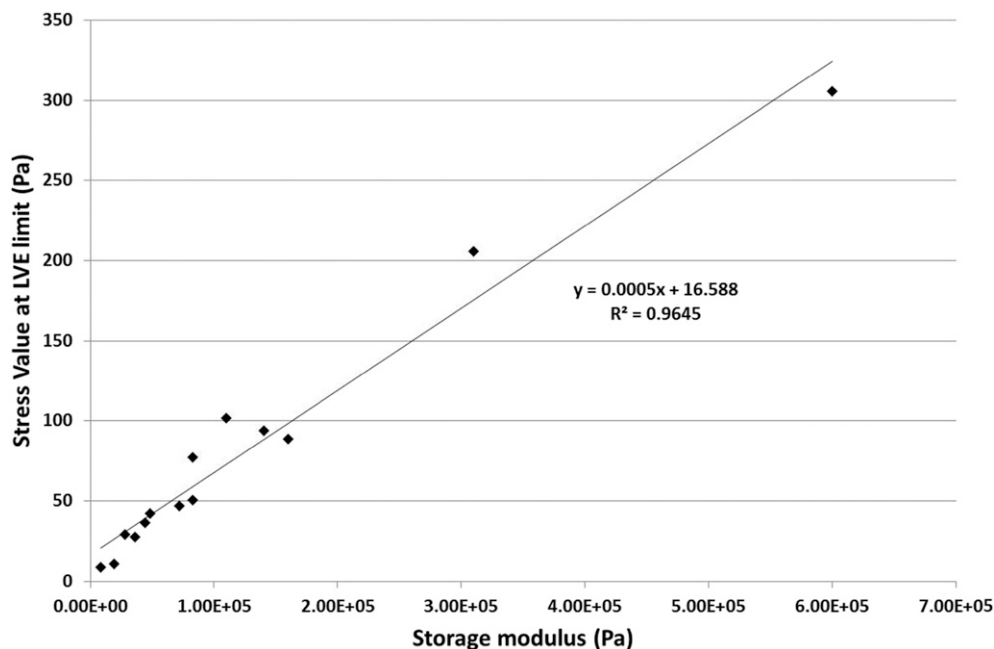
Figure 6. Correlation between storage modulus and stress values at the limit of LVE.

Accordingly, the separation percent and spreadability test results are directly proportional; the higher separation percent indicates lower viscosity of samples and, consequently, higher spreadability results. Nevertheless, for a physically stable formulation, we always need an optimum value that balance between easy application and spreadability of product and low phase separation during shelf life storage.

CONCLUSION

An optimum stable Dead Sea mud–based formulation composition requires the addition of thickeners. In addition, humectants such as glycerin can also improve spreadability.

Kaolin could not be used as a sole thickener in mud formulations to avoid color changes during shelf life. On the other hand, Natrosol® HHX 250 has the advantage of low concentration required to get the desired product viscosity; however, the problem of gritty texture encountered on using Natrosol® HHX 250 should be overcome, probably by modifying its incorporation procedure.

Ethanol at 5% (w/w) concentration level improved drying percent and extrudability, which are preferable aesthetic properties.

Separation percent at initial time point in the range of 5–10% appears to ensure minimal phase separation during product shelf life. Separation percent and spreadability can be correlated to products' rheological elastic parameters and yield stress values.

Casson and Herschel–Bulkley models were observed to describe the rheological data of Dead Sea mud formulations adequately. Yield stress, storage modulus, and viscosity at
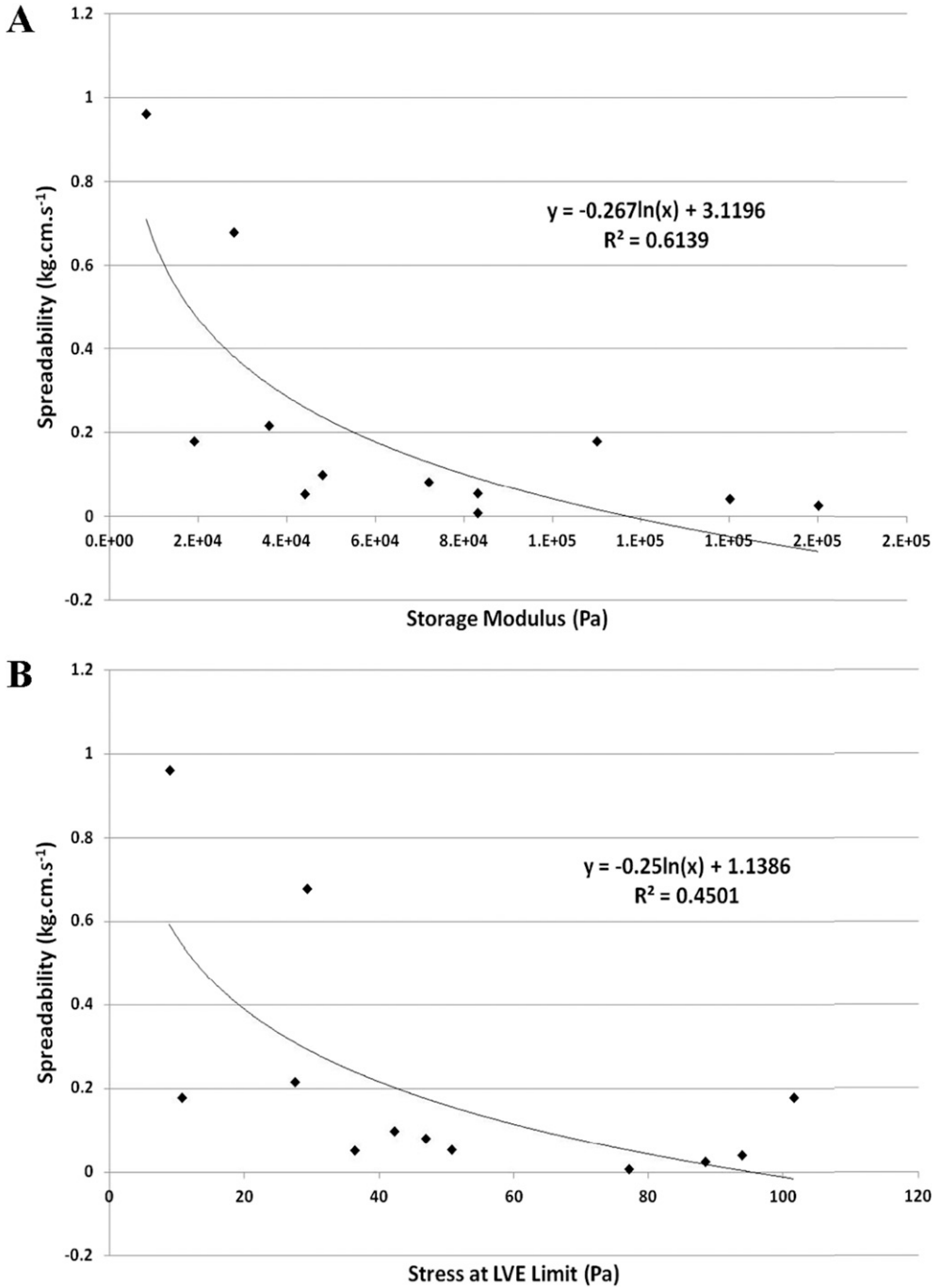
A

$y = -0.267\ln(x) + 3.1196$
$R^2 = 0.6139$

B

$y = -0.25\ln(x) + 1.1386$
$R^2 = 0.4501$

Figure 7. Correlation between spreadability and storage modulus value (A) and correlation between spreadability and stress values at the limit of LVE (B).
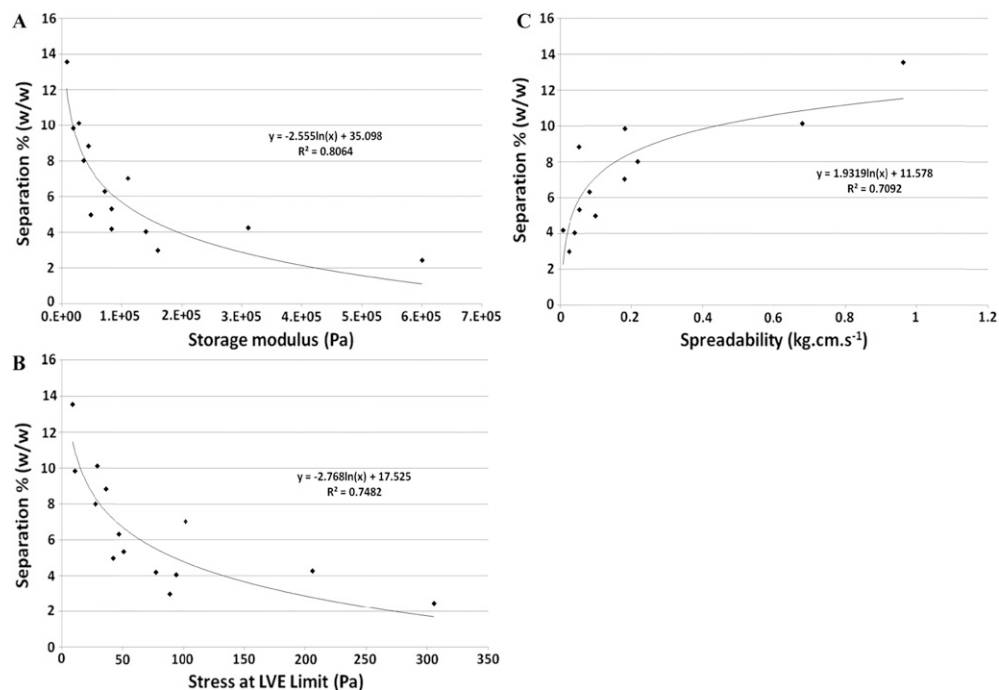
Figure 8. Correlation between separation percent (w/w) and storage modulus values (A), stress values at the limit of LVE (B), and spreadability values (C).

low shear rate values are the main rheological parameters that can be used to compare different formulations and record the changes during stability studies.

The best formulations from all physical criteria and stability aspects were B10G and K5B5G either with {1% and 5% (w/w)} or without ethanol. Their color was dark gray and they had showed no color changes during stability study. They were easily extrudable and had the best spreading behavior for the in-house products. Separation percent was moderate (5–10%), which was considered the best separation percent for mud preparations at initial time points necessary to avoid significant phase separation on storage. In addition, both formulas showed a typical viscoplastic, shear thinning behavior and were fitted to both models with good correlation coefficient.

Optimum values of rheological parameters, spreadability, and separation percent are always required, to balance between product stability, aesthetic acceptance, and easy application.

REFERENCES

(1) A. Abdel-Fattah and N. Pingitore Jr, Low levels of toxic elements in Dead Sea black mud and mud derived cosmetic products, *Environ. Geochem. Health.*, **31,** 487–492 (2009).

(2) Z. Ma'or, Y. Henis, Y. Alon, E. Orlov, E. Sorensen, and A. Oren, Antimicrobial properties of Dead Sea black mineral mud, *Int. J. Dermatol.*, **45,** 504–511 (2006).

(3) B. Abu-Jdayil and H.A. Mohameed, Facial mask comprising Dead Sea mud, *J. Cosmet. Sci.*, **57,** 441–454 (2006).

(4) A. Khlaifata, O. Al-Khashmanb, and H. Qutoba, Physical and chemical characterization of Dead Sea mud, *Mater. Charact.*, **61,** 564–568 (2010).

(5) Z. Ma'or, S. Yehuda, S. Magdassi, G. Meshulam-Simon, Y. Gavrieli, Z. Gilad, and D. Efron, *Cream Composition Comprising Dead Sea Mud*, United States Patents, Patent no. US 6,582,709 B1 (2003).

(6) B. Abu-Jdayil and H. Mohameed, Rheology of Dead Sea shampoo containing the antidandruff climbazole, *Int. J. Cosmetic Sci.*, **26,** 281–289 (2004).

(7) F. Veniale, A. Bettero, P. Jobstraibizer, and M. Setti, Thermal muds: Perspectives of innovations, *Appl. Clay Sci.*, **36,** 141–147 (2007).

(8) B. Abu-Jdayil, H. Mohameed, and A. Bsoul, Determination of optimal Dead Sea salt content in a cosmetic emulsion using rheology and stability measurements, *J. Cosmet. Sci.*, **59,** 1–14 (2008).

(9) V. Zague, D. Silva, A. Baby, A. Kaneko, and M. Velasco, Clay facial masks: Physicochemical stability at different storage temperatures, *J. Cosmet. Sci.*, **58,** 45–51 (2007).

(10) A. Garg, D. Aggarwal, S. Garg, and A. Singla, Spreading of semisolid formulations—An update, *Pharm. Technol.*, 84–105 (2002).

(11) K. Purushothamrao, K. Khaliq, P. Sagare, K. Patil, S. Kharat, and K. Alpana, Formulation and evaluation of vanishing cream for scalp, *Int. J. Pharma Sci. Tech.*, **4,** 32–41 (2010).

(12) R. Vieira, A. Fernandes, T. Kaneko, V. Consiglieri, C. Pinto, C. Pereira, A. Baby, and M. Velasco, Physical and physicochemical stability evaluation of cosmetic formulations containing soybean extract fermented by *Bifidobacterium animalis*, *Braz. J. Pharm. Sci.*, **45,** 515–525 (2009).

(13) T. Mezeger, *The Rheology Handbook: For Users of Rotational and Oscillatory Rheometers.* (Vincentz Verlag, Hanover, 2002).

(14) A. Garakani, N. Mostoufi, F. Sadeghi, M. Hosseinzadeh, H. Fatourechi, M. Sarrafzadeh, and M. Mehrnia, Comparison between different models for rheological characterization of activated sludge, *Iran J. Environ. Health Sci. Eng.*, **8,** 255–264 (2011).

(15) S. Balaghi, M. Mohammadifar, A. Zargaraan, H. Gavlighi, and M. Mohammadi, Compositional analysis and rheological characterization of gum tragacanth exudates from six species of Iranian *Astragalus*, *Food Hydrocolloid.*, **25,** 1775–1784 (2011).

(16) S. Livescu, Mathematical modeling of thixotropic drilling mud and crude oil flow in wells and pipelines—A review. *J. Petrol. Sci. Eng.*, **98–99,** 174–184 (2012).

(17) V. Kelessidis, R. Maglione, C. Tsamantaki, and Y. Aspirtak, Optimal determination of rheological parameters for Herschel–Bulkley drilling fluids and impact on pressure drop, velocity profiles and penetration rates during drilling, *J. Petrol. Sci. Eng.*, **53,** 203–224 (2006).

(18) R. P. Chhabra, "Non-Newtonian Fluids: An Introduction," in *Rheology of Complex Fluids*, A. Deshpande, J. Murali Krishnan, and P. Sunil, Eds. (Kumar & Springer, Munich 2010) pp. 1–33.

(19) A. Besq, C. Malfoy, A. Pantetb, P. Monneta, and D. Righi, Physicochemical characterisation and flow properties of some bentonite muds, *Appl. Clay Sci.*, **23,** 275–286 (2003).

(20) P. Herh, J. Tkachuk, S. Wu, M. Bernzen, and B. Rudolph, The rheology of pharmaceutical and cosmetic semisolids, *Am. Lab.*, Application Note (1998).

(21) S. Colo, P. Herh, N. Roye, and M. Larsson, Rheology and the texture of pharmaceutical and cosmetic semisolids. *Am. Lab.*, Application Note (2004).

(22) S. Emeish, Production of natural β-carotene from *Dunaliella* living in the Dead Sea. *JJEES*, **4,** 23–27 (2012).